



Original Article

Permanent disposal of Cs ions in the form of dense pollucite ceramics having low thermal expansion coefficient

Mia Omerašević^{a,*}, Miodrag Lukić^b, Marjetka Savić-Biserčić^c, Andrija Savić^d,
Ljiljana Matović^a, Zvezdana Baščarević^d, Dušan Bučevac^a

^a University of Belgrade, Vinca Institute of Nuclear Sciences, Department of Materials Science, PO Box 522, 11001, Belgrade, Serbia

^b Institute of Technical Sciences of the Serbian Academy of Sciences and Arts, Knez Mihailova 35/IV, Belgrade, Serbia

^c University of Belgrade, Vinca Institute of Nuclear Sciences, Chemical Dynamics Laboratory, PO Box 522, 11001 Belgrade, Serbia

^d University of Belgrade, Institute for Multidisciplinary Research, 11000, Belgrade, Serbia

ARTICLE INFO

Article history:

Received 25 December 2018

Received in revised form

9 June 2019

Accepted 1 July 2019

Available online 2 July 2019

Keywords:

Cs disposal

Ion exchange

Zeolite

Hot pressing

Thermal expansion

ABSTRACT

A promising method for removal of Cs ions from water and their incorporation into stable crystal structure ready for safe and permanent disposal was described. Cs-exchanged X zeolite was hot-pressed at temperature ranging from 800 to 950 °C to fabricate dense pollucite ceramics. It was found that the application of external pressure reduced the pollucite formation temperature. The effect of sintering temperature on density, phase composition and mechanical properties was investigated. The highest density of 92.5 %TD and the highest compressive strength of 79 MPa were measured in pollucite hot-pressed at 950 °C for 3 h. Heterogeneity of samples obtained at 950 °C was determined using scanning electron microscopy. The pollucite hot-pressed at 950 °C had low linear thermal expansion coefficient of $\sim 4.67 \times 10^{-6} \text{ K}^{-1}$ in the temperature range from 100 to 1000 °C.

© 2019 Korean Nuclear Society, Published by Elsevier Korea LLC. This is an open access article under the CC BY-NC-ND license (<http://creativecommons.org/licenses/by-nc-nd/4.0/>).

1. Introduction

Radioactive isotopes of cesium (Cs) are the major components of intermediate level radioactive wastes from nuclear power plants [1]. They belong to the most hazardous radiotoxic elements and therefore present a serious environmental problem. Cesium isotopes can migrate easily through groundwater to biosphere owing to the long half-life and high solubility in water [2,3]. Therefore, it is of great importance to remove and safely dispose radioactive Cs from the waste streams and prevent from entering soil and groundwater. One of the most effective procedures consists of two steps. The first step is removal of Cs cations from water, usually by ion exchange, whereas the second step is blocking of Cs cations inside of matrix [4–6]. Resins, which are typical organic exchangers, turned out to be unsuitable for this application due to their low thermal stability and potential swelling. Namely, resins containing Cs cations are normally mixed with bitumen or concrete in order to make solid blocks. The bituminization process as well as

concrete curing are accompanied by an increase in temperature causing swelling of the resins in the solidified products which can lead to a breakdown of the waste blocks and an increased leaching of radionuclides from the products [7].

On the other hand, zeolites, which are inorganic ion exchangers, consist of three-dimensional cage-structure made of aluminosilicate, showing high resistance to radioactive irradiation [8] and high affinity for Cs cations [1,8]. These properties make zeolite suitable material for the immobilization of radioactive cesium. Similar to resins, after ion-exchange it is essential to block the Cs ions into zeolite matrix and prevent their leaching when zeolite is in contact with water.

Different approaches have been applied in order to avoid leaching. For instance, zeolites loaded with Cs radioactive isotopes can be incorporated into borosilicate glass [9], cement [10] and glass [11]. Also, the pores of zeolites can be blocked with barium [12,13]. However, despite the presence of these matrices, the Cs will slowly diffuse through the matrix and eventually contaminate groundwater.

One of the promising methods for trapping Cs radioisotopes into a zeolite framework is based on thermal treatment of zeolite conducted after ion exchange and its phase transformation into

* Corresponding author. Vinca Institute of Nuclear Sciences, PO Box 522, 11001, Belgrade, Serbia.

E-mail address: mia@vinca.rs (M. Omerašević).

structurally new, crystalline phase which is denser than the starting zeolite structure [14–21]. A number of studies suggest that pollucite is one of the most stable phases under depository conditions and is a preferable phase for Cs immobilization [1,22–26]. Although pollucite is commonly defined as a feldspathoid, it is actually a cesium aluminosilicate belonging to the analcime zeolite family [27,28] with ideal formula $(\text{Cs}, \text{Na})_{16}\text{Al}_{16}\text{Si}_{32}\text{O}_{96} \cdot n\text{H}_2\text{O}$ [23]. Framework structure of pollucite consists of 48 $(\text{Si}, \text{Al})\text{O}_4$ tetrahedra and 16 Cs^+ ions in 12-coordinated sites surrounded by the framework [6]. The space group of this mineral is cubic Ia3d with cell parameter of $\sim 13.68 \text{ \AA}$ [29]. Pollucite is one of the potential final storage options for radioactive Cs owing to its specific structure. It has appropriately sized channels which tightly hold Cs ions inside of pollucite structure. Therefore, the removal of Cs would require a considerable energy necessary to destroy the pollucite framework [30].

The aim of this work is to transform Cs-exchanged X zeolite powder into stable ceramics using hot pressing. Zeolite X is the sodium form of synthetic faujasite (or Na-FAU). The framework of X-type zeolite consists of sodalite cages which are connected through hexagonal prisms. The effective width of the 12-membered ring channel in faujasite is 7.4 \AA , assuming the diameter of O to be 2.7 \AA . The main cavities in the structure of X-zeolite are nearly spherical (elliptical) in shape with diameter of $\sim 13 \text{ \AA}$. They are called supercages and are surrounded by 10 sodalite cages [31,32].

Based on our previous study, it is believed that hot pressing of Cs-exchanged X zeolite powder might be an efficient way to immobilize radioactive Cs by its incorporation into crystal lattice of stable pollucite [33]. The previous study showed that hot pressing of Cs-exchanged form of Na, Ca-LTA type of zeolite resulted in formation of pollucite with improved resistance to Cs leaching.

In this study a special attention will be given to the thermal expansion coefficient of pollucite. This thermal property might be of great importance for safe disposal knowing that β -decay causes heating of waste forms during the first 500 years of waste storage [34]. Since all of Cs radioisotopes are beta emitters (β^-) significant heating is possible after waste emplacement in a repository. Therefore, solid waste form can generate enough self-heat from decays to result in an initial storage temperature as high as $600 \text{ }^\circ\text{C}$ which can cause considerable expansion of waste. Therefore, it is important to examine thermal expansion coefficient of obtained solid pollucite ceramics as it determines the stability of obtained waste blocks.

2. Experimental procedure

2.1. Materials

The sodium form of X (FAU) type ($\text{Si}/\text{Al} = 1.26$) zeolite was used as a starting material and denoted as Na-X. Partially exchanged Cs^+ form of Na-X type of zeolite was prepared after 3 successive exchanges from 0.25 M CsCl solutions (Cesium Chloride p.a., VWR AnalaR NORMAPUR[®], min 99.5% CsCl) with the solid/liquid ratio 1/20 (see Fig. 1a). The percentage of exchanged Na cations was determined based on the difference between Na concentration in zeolite prior to and after the ion exchange.

At the end of the exchange procedure, Cs-exchanged X form of zeolite, hereafter Cs-X, was washed with distilled water (in order to remove Cl) and dried at $60 \text{ }^\circ\text{C}$ before hot pressing (see Fig 1a).

Hot pressing of Cs-X powder was carried out in hot press (Astro Industries, California, USA) equipped with graphite heating element at temperature ranging from 800 to $950 \text{ }^\circ\text{C}$ using graphite mould with internal diameter of 10 mm (see Fig. 1b). The furnace was filled with argon in order to protect graphite from oxidation.

Samples were heated to the final sintering temperature at heating rate of $10 \text{ }^\circ\text{C min}^{-1}$ and held for 3 h under mechanical pressure of 35 MPa . The applied mechanical pressure was limited by the strength of graphite used to manufacture mould and pistons.

2.2. Methods of characterization

X-Ray Fluorescence Spectrometry (XRF) analysis of zeolite powders before (NaX) and after ion exchange (CsX) was performed using a Thermo Scientific ARL Perform'X Sequential X-Ray Fluorescence Spectrometer equipped with a Rh target tube, seven monochromators and a wavelength-dispersive spectrometer. Na-X and Cs-X powders were mixed with boric acid and mechanically pressed into pellets having a diameter of 25 mm and height of 3.6 mm . The experiments were conducted under vacuum in order to avoid interaction of X-rays with air particles. The data were acquired and processed using Thermo Scientific UniQuant Analysis Software. The elemental compositions of Na-X and Cs-X were calculated based on the oxide weight fractions in anhydrous zeolite. Particle size distribution of CsX powder was measured by laser diffraction using Horiba LA-920.

All samples were also investigated by X-ray powder diffraction (XRPD). XRPD patterns were obtained by Rigaku Ultima IV diffractometer, using a Cu tube operated at 40 kV and 40 mA . Hot-pressed samples were crushed and pulverized using alumina mortar and pestle. The obtained powders as well as zeolite powders were loaded on horizontal holder. The diffraction data of samples were collected in 2θ range from 4 to 65° using a scan speed of 1° min^{-1} and a step size of 0.02° , for routine phase analysis. The amounts of present phases were estimated using PDLX2 program. The density and open porosity of hot-pressed samples were determined by the Archimedes' method using water as immersion liquid. The theoretical density was calculated according to the rule of mixtures, based on density of natural pollucite of 2.94 g cm^{-3} [29] and density of nepheline of 2.63 g cm^{-3} [35]. The thermal behavior of the Cs-X zeolite was investigated by simultaneous differential thermal analysis and thermogravimetry (DTA/TG) using the instrument Setsys Evolution, Setaram, France. Zeolite samples were analyzed at a heating rate of $10 \text{ }^\circ\text{C min}^{-1}$, in air atmosphere at a flow rate of $90 \text{ cm}^3 \text{ min}^{-1}$. Morphological analysis of Cs-X zeolite before and after the heat treatments was performed using VEGA TS 5130 MM scanning electron microscope (SEM). The samples were coated with thin layer of gold and the secondary electron images were acquired using beam of electrons accelerated at 20 and 30 kV . Polished samples were coated with a thin layer of gold and examined by scanning electron microscopy in a back-scatter mode as well as electron dispersive spectroscopy (EDS). Room-temperature compressive test of six samples was carried out by 1185 Instron-type testing machine at a strain rate of 2 mm min^{-1} . The average compressive strength value was calculated. Two end surfaces of the cylindrical samples were carefully ground to make them parallel. The thermal expansion behavior of hot-pressed pollucite was investigated in the temperature range from 100 to $1000 \text{ }^\circ\text{C}$ by the means of dilatometer BÄHR Thermoanalyse GmbH, Germany at rate of $2 \text{ }^\circ\text{C min}^{-1}$.

3. Results and discussion

SEM micrograph shown in Fig. 2 reveals that Cs-X powder consists of agglomerates of irregular shape having diameter ranging from 2 to $5 \text{ }\mu\text{m}$. These agglomerates are mainly composed of small particles having diameter from 0.15 to $0.4 \text{ }\mu\text{m}$. Fig. 3 shows bimodal particle size distribution of Cs-X powder with two peaks located around 0.25 and $4 \text{ }\mu\text{m}$. Apparently, ultrasound breaks Cs-X particles down into smaller, submicron, particles. On the other side,

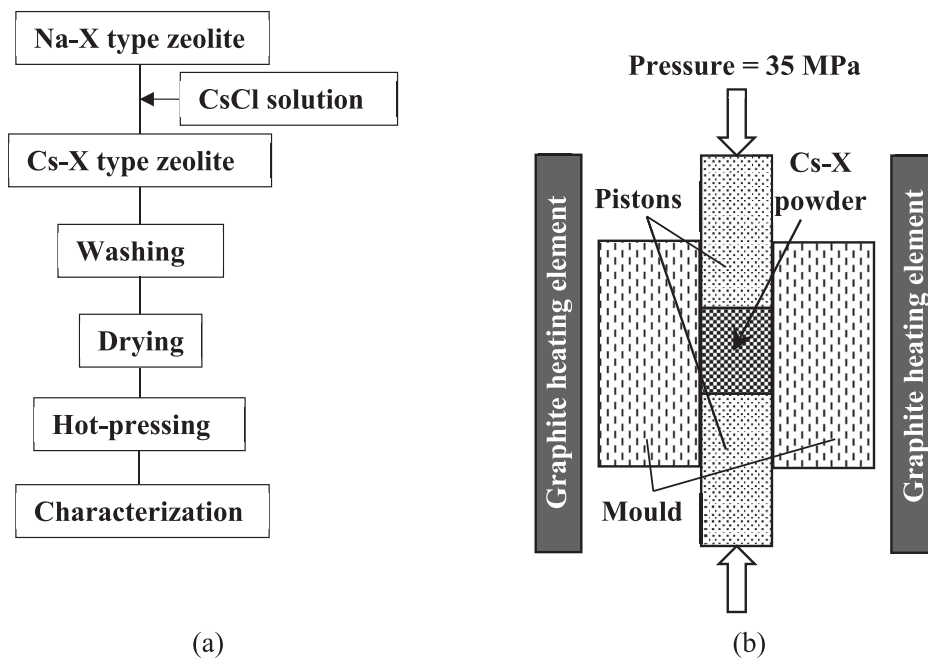


Fig. 1. Schematics of a) experimental procedure and b) hot pressing of Cs-X powder.

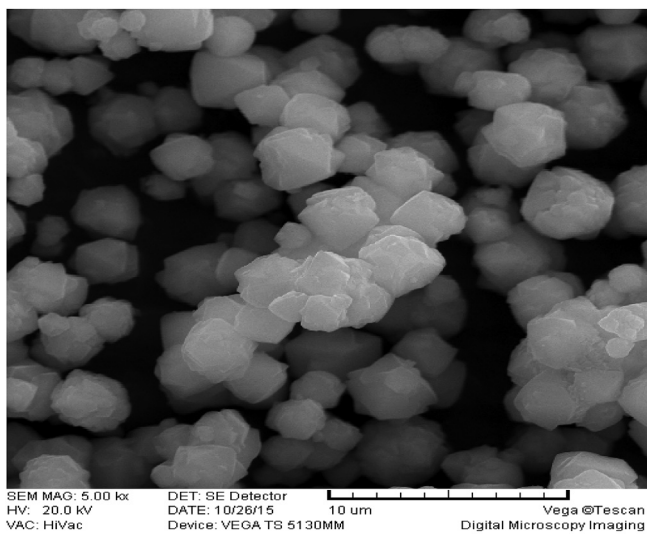


Fig. 2. SEM micrograph of Cs-X zeolite powder.

coarser Cs-X particles with diameter as large as 10 μm are present as well.

The chemical composition of Na-X zeolite before and after an exchange with Cs⁺ ions as well as the quantities of exchangeable cations (mainly Na) are determined and presented in Table 1. During the ion-exchange process, more than half of initial sodium ions (66%) are replaced with Cs ions. It is important to stress that the true attained exchange level is somewhat higher than 66%. There is usually a certain number of cations in zeolites that cannot be exchanged. For this reason, zeolites are normally characterized by cation exchange capacity [36] which shows how many cations can be exchanged (total exchange). However, neither cation exchange capacity nor the exchange reaction $\text{Na}^+ \rightleftharpoons \text{Cs}^+$ was studied in detail as the main goal of our work was synthesis of dense polycrystalline ceramics.

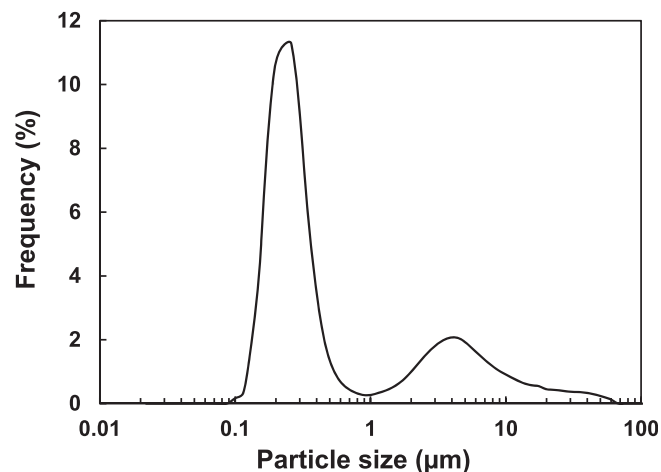


Fig. 3. Particle size distribution of Cs-X powder.

As can be seen from the results of XRF analysis presented in Table 1, the obtained cesium form of the zeolite contains 32.66 wt% of Cs⁺ ions.

XRPD patterns of Na-X zeolite before and after ion exchange are presented in Fig. 4. The replacement of Na ions with Cs in the zeolite structure results in the formation of Cs-X zeolite. As can be seen from Fig. 4, two peaks characteristic of starting Na-X, located at $2\theta = 15.43^\circ$ and 20.13° completely disappeared while the intensity of peaks located at $2\theta = 25.40^\circ$ and 29.19° increased in Cs-X form. These peaks are, cation-sensitive peaks which are very strong in the Cs-form while very weak in the Na-form [37].

The change of weight and thermal effects during the heating of Cs-X powder to 1200 °C were recorded by TG-DTA analysis and presented in Fig. 5. The weight loss of ~16% observed on TG curve in temperature range from room temperature to 300 °C is attributed to desorption of adsorbed water. The desorption is an endothermic process which was also confirmed by the pronounced endothermic deviation of DTA curve accompanying the weight loss and having a

Table 1
Elemental composition of Na-X zeolite before and after Cs⁺ exchange.

Elements (wt%)	Na	Mg ^a	Al	Si	K ^a	Ca ^a	Fe ^a	Cs	O
Before exchange	13.93 ± 0.13	0.07	18.05 ± 0.12	21.88 ± 0.11	0.03	0.02	0.02	0.00 ± 0.00	45.99 ± 0.26
After exchange	4.73 ± 0.09	0.01	16.22 ± 0.11	18.39 ± 0.12	0.01	0.01	0.01	32.66 ± 0.23	27.99 ± 0.24

^a Estimated error is less than 0.01 wt%.

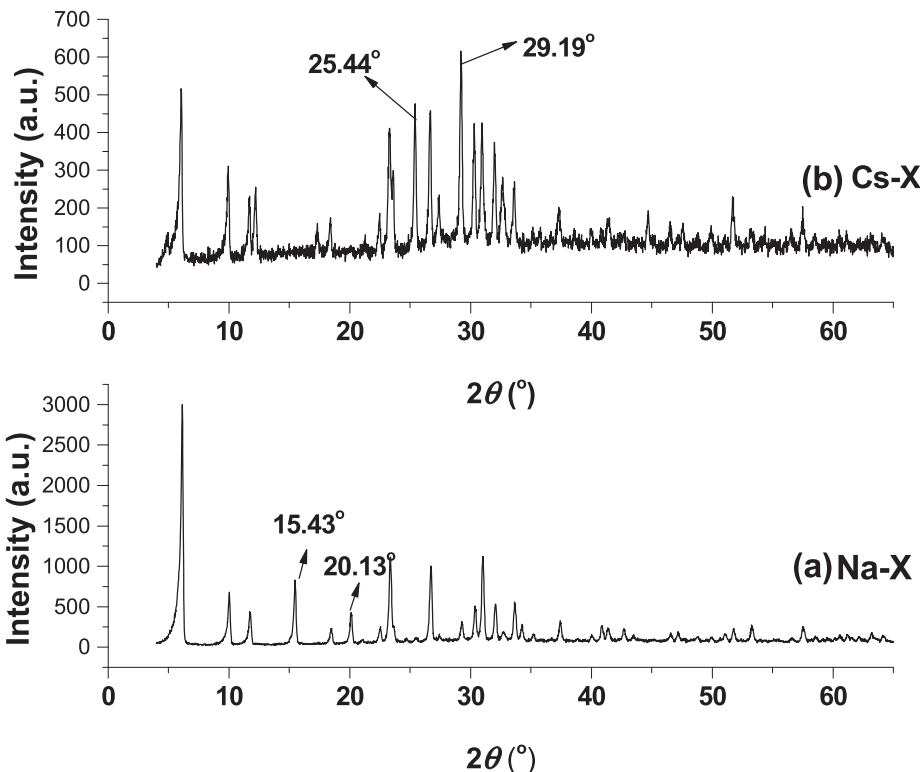


Fig. 4. XRPD patterns of a) raw Na-X type zeolite and b) Cs-X.

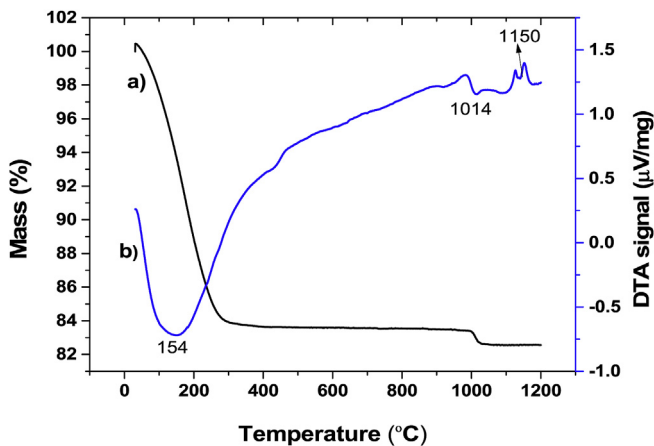


Fig. 5. Simultaneous a) TG and b) DTA curves of Cs-X sample.

minimum at the temperature of 154 °C. The small weight loss of ~1% which takes place in the very narrow temperature range 995 °C–1030 °C is ascribed to the loss of structural water. The exact nature of this water is as yet unknown but may perhaps be described as residual OH attached to lattice relics [38]. Similar to loss of adsorbed water, the loss of structural water is accompanied

by small endothermic deviation of DTA curve having a minimum at 1014 °C. The small oscillations of DTA curve at temperatures above 1030 °C are not accompanied by measurable weight loss. The XRPD analysis previously obtained by Dimitrijevic et al. [16] and the XRPD analysis of hot-pressed samples obtained in this work (Fig. 6) suggest that these deviations may be attributed to the structural changes such as transformation of zeolite structure into amorphous and/or crystalline phase which takes place above 1000 °C.

DTA/TG analysis was performed in order to estimate the temperature at which the amorphous structure transforms into the new crystalline structure. As already known from previous studies, the use of hot pressing not only reduces the temperature necessary to achieve high density but also reduces the temperature of formation of the new crystalline phase in exchanged zeolite for 250 °C when compared to pressureless sintering [33,39]. Bearing in mind that pollucite powder was obtained from Cs-X zeolite powder after calcination at 1100 °C [40] it is expected that in this study the pollucite phase can be obtained at temperature as low as 850 °C. This was confirmed by XRPD analysis presented in Fig. 6 which shows that the structure of the Cs-X zeolite transforms into amorphous phase after hot pressing at 800 °C (pattern a). It is believed that heating to 800 °C leads to breaking of T-O-T bridges (T = Si, Al) which causes a collapse of the zeolite structure and formation of the amorphous intermediate product [15]. Further increase in temperature to 850 °C causes recrystallization of the

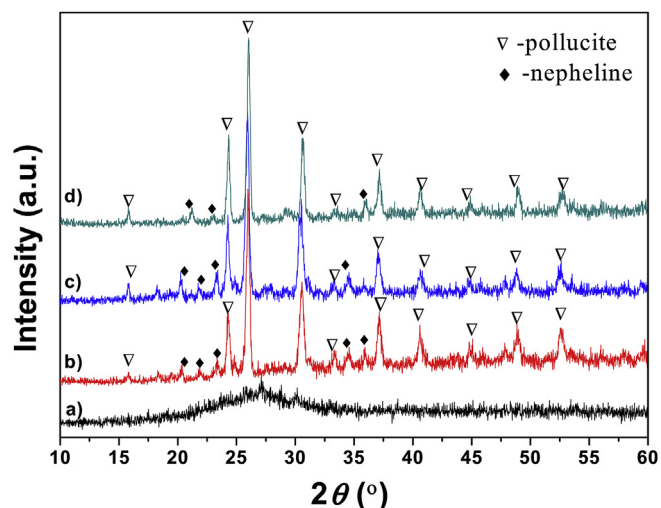


Fig. 6. XRPD patterns of Cs-X hot-pressed at a) 800 °C, b) 850 °C, c) 900 °C and d) 950 °C.

sample, and formation of two phases: dominant pollucite phase (pollucite syn.jcpds 29–0407) and minor nepheline phase (jcpds 35–0424) with characteristic peaks at $2\theta = 21.31^\circ$ and 23.00° (pattern b). Therefore, the final stage of this thermal transformation includes the polymorphous transformation into more stable crystalline phases. As Fig. 6 shows, both phases, pollucite and nepheline, stayed stable even after hot pressing at 950 °C (patterns c and d). The appearance of the nepheline phase ($\text{NaAl}(\text{SiO}_4)$) is quite expected and justified by the fact that a certain amount of Na ions was not exchanged with Cs ions and that it remains in the zeolite structure. According to Table 1, 66% of Na ions were replaced with Cs ions.

From the thermodynamic point of view, the decrease in temperature of transformation of Cs-X zeolite into pollucite by simultaneous application of high temperature and external pressure can be explained by Clausius-Clapeyron equation, as described in our previous work [33,39].

It is also important to note the splitting of XRPD peaks characteristic for pollucite, especially those in the XRPD patterns recorded for samples hot-pressed at 900 and 950 °C. As Fig. 6 shows, XRPD patterns denoted as c) and d) possess peaks located at $\sim 31^\circ$ which are split in two or even three peaks. This indicates the presence of phases with similar crystal structure and small difference in unit cell parameters. Therefore SEM (BSE mode) and EDS analysis were employed to analyze the phases present at the polished surface of sample hot-pressed at 950 °C. SEM micrograph of sample hot-pressed at 950 °C taken in back scattered electron (BSE) mode is presented in Fig. 7 which clearly shows the heterogeneity of the sample. The heterogeneity might be the result of the presence of Na-enriched and Cs-enriched domains of pollucite as previously observed by Teertstra et al. [41]. The results of EDS analysis of sample hot-pressed at 950 °C are presented in Table 2, which shows the concentration of detected elements. The largest ratio between maximum and minimum concentration of particular element was measured for Na and Cs. Combining results presented in Table 2 and locations of EDS analysis given in Fig. 7 one can conclude that there are three pollucite phases, $(\text{Cs}, \text{Na})_{16}\text{Al}_{16}\text{Si}_{32}\text{O}_{96}$, with different concentration of Na and Cs and nepheline phase. Dark phase represented by spectra 1, 2, 3 and 4 is pollucite containing the largest concentration of Na (6.08–6.68 wt%) and the lowest concentration of Cs (18.19–19.94 wt%). On the other side, the bright phase represented by spectra 5, 6, 7, 8, 9 is pollucite containing the lowest

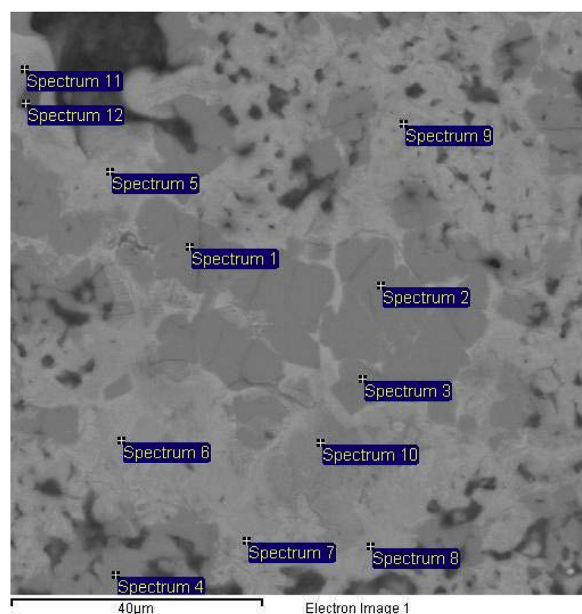


Fig. 7. SEM-BSE micrograph of polished surface of pollucite hot-pressed at 950 °C showing the locations where EDS analysis was conducted. The results of EDS analysis are presented in Table 2.

Table 2
Results of EDS analysis of sample hot-pressed at 950 °C.

Spectrum	O	Na	Al	Si	Ca	Cs
1	44.56	6.41	11.97	16.77	0.35	19.94
2	46.58	6.08	11.71	15.94	0.00	19.69
3	47.93	6.13	11.16	14.94	1.66	18.19
4	49.37	6.68	11.88	12.71	0.51	18.86
5	44.71	2.58	10.16	13.63	0.33	28.59
6	44.66	4.02	10.31	13.93	0.00	27.09
7	45.35	3.73	10.00	13.78	0.44	26.70
8	43.95	3.95	10.43	13.85	0.27	27.56
9	41.55	3.44	10.43	14.34	0.34	29.91
10	46.40	5.25	11.12	15.07	0.60	21.56
11	47.40	3.64	10.91	14.43	0.64	22.98
12	45.53	17.15	19.92	15.36	0.00	2.04

concentration of Na (2.58–4.02 wt%) and the largest concentration of Sr (26.70–29.91 wt%). There is also the third phase represented by spectra 10 and 11 containing median concentrations of Na (3.64–5.25 wt%) and Sr (21.56–22.98 wt%). The color of this phase is between bright and dark. Finally, the black phase represented by spectrum 12 is nepheline. Although nepheline is not expected to contain Cs, Table 2 indicates the presence of small amount of Cs of 2.04 wt%. The presence of small amount of Cs might be the result of the background signal originating from surrounding pollucite phase reach in Cs. Based on these results, it can be concluded that partitioning of Na and Cs takes place during sintering of Cs-X zeolite.

Fig. 8 shows the change of open porosity and compressive strength of hot-pressed samples with sintering temperature. Sintering temperature was limited to 950 °C since the higher temperature causes considerable weight loss due to matter evaporation. As Fig. 8 evidences, porosity decreases with sintering temperature due to faster sintering process at higher temperature. As expected, the decrease in porosity is followed by the increase in compressive strength. As can be seen in Fig. 8, samples sintered at 950 °C possess the highest strength of 79 MPa and the highest density of 2.71 g cm^{-3} (Table 3.). This result is quite expected

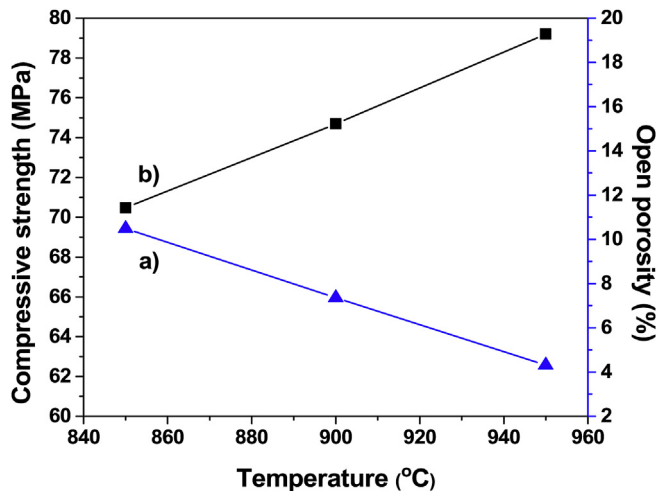


Fig. 8. Effect of sintering temperature on a) open porosity and b) compressive strength of hot-pressed samples.

Table 3
Density of samples hot-pressed at different temperature.

Temperature (°C)	Density (g cm ⁻³)	Relative density (%TD)
850	2.180	74.35
900	2.484	84.72
950	2.710	92.49

knowing that high temperature accelerates sintering process and therefore improves density. As mentioned, the samples sintered at 950 °C consist of two phases; pollucite and nepheline. Therefore, the theoretical density (TD) of these samples was calculate by applying the rule of mixture. According to the XRPD analysis, the fractions of pollucite and nepheline were found to be 91 and 9 wt%, respectively. The amounts of present phases were roughly estimated by comparing the intensities of characteristic peaks with the help of PDLX2 program and assuming that there was no amorphous phase. The absence of substantial amount of amorphous phase was confirmed by XRPD patterns (Fig. 6) having low and quite flat base line as well as detailed EDS analysis (Fig. 7) identifying pollucite and nepheline. Based on this it was calculated that the relative density of samples sintered at 950 °C was 92.49 %TD. The samples with the highest compressive strength, i.e., samples sintered at 950 °C were analyzed in the following section.

The secondary electron SEM image given in Fig. 9 shows a fracture surface of pollucite sample hot-pressed at 950 °C. The observed fracture surface is typical for brittle material showing both, transgranular and intergranular fracture mode. The majority of grains fracture transgranularly whereas just few of them deflect crack or undergo pull-out (Fig. 9). Small number of grains undergoing pull-out is normally ascribed to strong grain interface and the lack of glassy phase normally located at the grain boundaries and triple junctions [42]. The pore radius was estimated to be below 4 μm. The pores are isolated which is very important feature when it comes to reduction of leaching rate. Detailed analysis of mechanical properties such as flexural strength and fracture toughness was not conducted as they do not play important role in waste disposal. Compressive strength of 79 MPa is sufficiently high to allow easy handling and disposal of pollucite in the form of stacks of several blocks.

As mentioned in the introduction section, it is well known that solid waste which contains radioactive Cs can generate enough self-heat from β-decay to result in an initial storage temperature as high

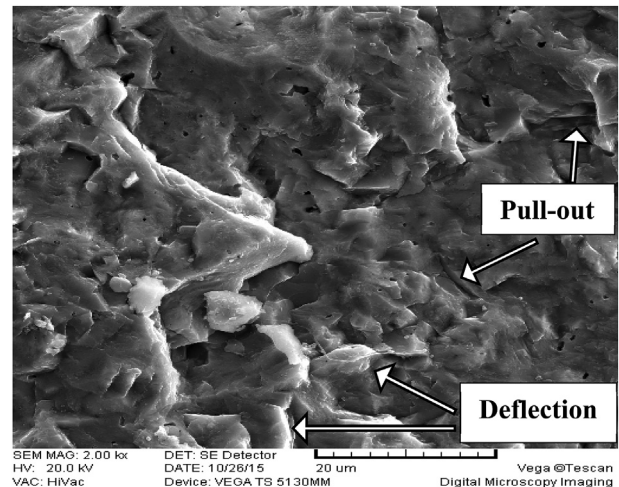


Fig. 9. SEM micrograph of fracture surface of pollucite hot-pressed at 950 °C.

as 600 °C. Even after 100 years of disposal the temperature may be still as high as 300 °C. Therefore, the host material is expected to expand due to increase in temperature. Thermal expansion property of dense pollucite obtained at 950 °C was examined in the following section.

Linear thermal expansion of dense pollucite obtained by hot pressing at 950 °C is presented in Fig. 10. It was found that the linear thermal expansion coefficient (TEC) in the temperature range 100–1000 °C was $4.67 \times 10^{-6} \text{ K}^{-1}$ which is a half of the value of cementitious materials [43]. It is already known that synthetic pollucite, free of impurities, may have a low thermal expansion coefficient. Yanase et al. [44] synthesized the pollucite porous body and obtained samples with thermal expansion coefficient of only $1.0 \times 10^{-6} \text{ K}^{-1}$ in temperature range 25–1000 °C. The reason for the higher value of thermal expansion coefficient of samples obtained in this study is the presence of ~9% of nepheline as minor phase which is known to have relatively high TEC of $\sim 1.6 \times 10^{-5} \text{ K}^{-1}$ [45].

The measured value of TEC of dense pollucite ($4.67 \times 10^{-6} \text{ K}^{-1}$) obtained in this work is satisfactory from the aspect of Cs ions disposal. This means that there is no considerable expansion of the pollucite during heating. Since the displacement is only 4.67 μm per meter per Kelvin, it can be calculated that 1 m long piece of

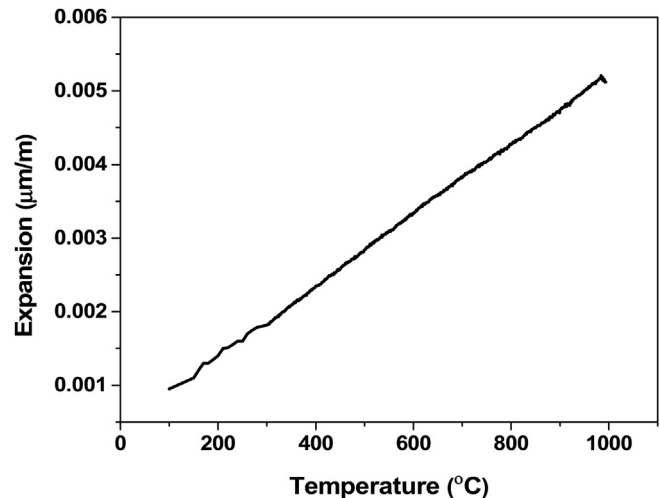


Fig. 10. Thermal expansion behavior of dense pollucite hot-pressed at 950 °C.

pollucite is going to expand only 2.8 mm when heated from room temperature to 600 °C. Therefore, it can be assumed that after 100 years of storage there will not be major changes in the material, i.e., the disruption of the existing structure and leaching of cesium ions.

4. Conclusion

Cs form of X zeolite containing more than 32 wt% of Cs ions was obtained after ion exchange. It was found that the structure of Cs-X zeolite powder compacts transformed into amorphous phase during hot-pressing at 800 °C. Further increase in hot-pressing temperature to 850 °C caused crystallization of amorphous phase into new, stable phase called pollucite which was accompanied by the presence of minor crystalline phase called nepheline. These phases remained stable at 950 °C. The samples hot-pressed at 950 °C had relative density of 92.49 %TD and the highest strength of 79 MPa. SEM-BSE micrograph of sample hot-pressed at 950 °C showed presence of two crystalline phases, pollucite and nepheline. Linear thermal expansion coefficient (TEC) measured in temperature range from 100 to 1000 °C was $4.67 \times 10^{-6} \text{ K}^{-1}$. The measured TEC value is considered to be relatively low and therefore is not expected to cause cracking of disposed radioactive material during heating due to radioactive decay. The absence of cracking is one of the main prerequisites for low Cs leaching rate. The main advantages of this method are its efficiency, low cost and environmental safety. It can be concluded that the obtained cesium aluminosilicate ceramics is a promising candidate for the permanent immobilization and safe disposal of Cs radionuclides.

Acknowledgments

This work was supported by the Ministry of education, science and technological development of the Republic of Serbia (project number: 45012).

References

- [1] P. Bosch, D. Caputo, B. Liguori, C. Colella, Safe trapping of Cs in heat-treated zeolite matrices, *J. Nucl. Mater.* 324 (2004) 183–188, <https://doi.org/10.1016/j.jnucmat.2003.10.001>.
- [2] R. Cortés-Martínez, M.T. Olguín, M. Solache-Ríos, Cesium sorption by clinoptilolite-rich tuffs in batch and fixed-bed systems, *Desalination* 258 (2010) 164–170, <https://doi.org/10.1016/j.desal.2010.03.019>.
- [3] S.S. Nenadović, M.T. Nenadović, I.S. Vukanac, M.O. Omerasević, L.M. Kljajević, Radiological hazards of ^{137}Cs in cultivated and undisturbed areas, *Nucl. Technol. Radiat. Protect.* 26 (2011) 115–118, <https://doi.org/10.2298/NTRP1102115N>.
- [4] I. Plecas, A. Peric, A. Kostadinovic, J. Drljaca, S. Glodic, Leaching behavior of ^{60}Co and ^{137}Cs from spent ion exchange resins in cement matrix, *Cement Concr. Res.* 327 (2004) 171–174.
- [5] I.B. Plecas, R.S. Pavlovic, S.D. Pavlovic, Leaching of ^{60}Co and ^{137}Cs from spent ion exchange resins in cement – bentonite clay matrix, *J. Nucl. Mater.* 327 (2004) 699–701, <https://doi.org/10.1016/j.jnucmat.2004.02.001>.
- [6] A. Dyer, D. Keir, Nuclear waste treatments by zeolites, *Zeolites* 4 (1984) 215–218, [https://doi.org/10.1016/0144-2449\(84\)90026-5](https://doi.org/10.1016/0144-2449(84)90026-5).
- [7] J.P. Aittola, J. Chyssler, H. Ringberg, Thermal Stability of Ion-Exchange Resins, *Studsvik Energitekn. AB*, 1982.
- [8] H. Mimura, T. Kanno, Processing of radioactive waste solution with zeolites (I): thermal-transformations of Na, Cs and Sr forms of zeolites, *Sci. Rept. Res. Inst.* 29 (1980) 102–111.
- [9] B.X. Gu, L.M. Wang, R.C. Ewing, Effect of amorphization on the Cs ion exchange and retention capacity of zeolite-NaY, *J. Nucl. Mater.* 278 (2000) 64–72, [https://doi.org/10.1016/S0022-3115\(99\)00224-X](https://doi.org/10.1016/S0022-3115(99)00224-X).
- [10] A.M. El-Kamash, M.R. El-Naggar, M.I. El-Dessouky, Immobilization of cesium and strontium radionuclides in zeolite-cement blends, *J. Hazard Mater.* 136 (2006) 310–316, <https://doi.org/10.1016/j.jhazmat.2005.12.020>.
- [11] J.M. Juoi, M.I. Ojovan, W.E. Lee, Microstructure and leaching durability of glass composite wasteforms for spent clinoptilolite immobilisation, *J. Nucl. Mater.* 372 (2008) 358–366, <https://doi.org/10.1016/j.jnucmat.2007.04.047>.
- [12] A. Dyer, K.Y. Mikhail, The use of zeolites for the treatment of radioactive waste, *Mineral. Mag.* 49 (1985) 203–210, <https://doi.org/10.1180/minmag.1985.049.351.07>.
- [13] M. Luo, M. Wen, J. Wang, J. Zhu, The study of cooperation solidification of Cs based on ZSM-5 zeolite, *Energy Procedia*. 39 (2013) 434–442, <https://doi.org/10.1016/j.egypro.2013.07.234>.
- [14] A. Radulović, V. Dondur, R. Dimitrijević, D. Arandjelović, Thermal transformation of Na-LTA zeolite into low-carnegieite: the influence of residual sodium and aluminium species, *Thermochim. Acta* 511 (2010) 37–42, <https://doi.org/10.1016/j.tca.2010.07.022>.
- [15] R. Dimitrijević, V. Dondur, A. Kremenović, Thermally induced phase transformations of Ca-exchanged LTA and FAU zeolite frameworks: rietveld refinement of the hexagonal $\text{CaAl}_2\text{Si}_2\text{O}_8$ diphylosilicate structure, *Zeolites* 16 (1996) 294–300, [https://doi.org/10.1016/0144-2449\(95\)00154-9](https://doi.org/10.1016/0144-2449(95)00154-9).
- [16] R. Dimitrijević, V. Dondur, N. Petranovic, The high temperature synthesis of CsAlSiO_4 -ANA, a new polymorph in the system $\text{Cs}_2\text{O}-\text{Al}_2\text{O}_3-\text{SiO}_2$, *J. Solid State Chem.* 345 (1991) 335–345.
- [17] B. Nedic, A. Kremenovic, V. Dondur, R. Dimitrijevic, Strontium deficient feldspar - structure and X - Ray powder diffraction line broadening analysis, *Cryst. Res. Technol.* 43 (2008) 266–272, <https://doi.org/10.1002/crat.200710974>.
- [18] M. Omerasević, J. Ružić, N. Vuković, U. Jovanović, M. Mirković, V. Maksimović, V. Dondur, Removal of Cs ions from aqueous solutions by using matrices of natural clinoptilolite and its safe disposal, *Sci. Sinter.* 48 (2016) 101–107, <https://doi.org/10.2298/SOS16011010>.
- [19] C. Ferone, B. Liguori, A. Marocco, S. Anaclerio, M. Pansini, Monoclinic (Ba, Sr)-celonian by thermal treatment of (Ba, Sr)-exchanged zeolite A, *Microporous Mesoporous Mater.* 134 (2010) 65–71, <https://doi.org/10.1166/asl.2017.9089>.
- [20] P. Cappelletti, G. Rapisardo, B. de Gennaro, A. Colella, A. Langella, S.F. Graziano, D.L. Bish, M. de Gennaro, Immobilization of Cs and Sr in aluminosilicate matrices derived from natural zeolites, *J. Nucl. Mater.* 414 (2011) 451–457, <https://doi.org/10.1016/j.jnucmat.2011.05.032>.
- [21] G.D. Gatta, A. Brundu, P. Cappelletti, G. Cerri, B. de Gennaro, M. Farina, P. Fumagalli, L. Guaschino, P. Lotti, M. Mercurio, New insights on pressure, temperature, and chemical stability of $\text{CsAlSi}_5\text{O}_{12}$, a potential host for nuclear waste, *Phys. Chem. Miner.* 43 (2016) 639–647, <https://doi.org/10.1007/s00269-016-0823-8>.
- [22] G.D. Gatta, F. Nestola, T.B. Ballaran, Elastic behavior, phase transition, and pressure induced structural evolution of analcime, *Am. Mineral.* 91 (2006) 568–578, <https://doi.org/10.2138/am.2006.1994>.
- [23] G.D. Gatta, R. Rinaldi, G.J. McIntyre, G. Nenert, F. Bellatreccia, A. Guastoni, G. Della Ventura, On the crystal structure and crystal chemistry of pollucite, $(\text{Cs,Na})_{16}\text{Al}_{16}\text{Si}_{32}\text{O}_{96} \cdot n\text{H}_2\text{O}$: a natural microporous material of interest in nuclear technology, *Am. Mineral.* 94 (2009) 1560–1568, <https://doi.org/10.2138/am.2009.3237>.
- [24] K. Yanagisawa, M. Nishioka, N. Yamasaki, Immobilization of cesium into pollucite structure by hydrothermal hot-pressing, *J. Nucl. Sci. Technol.* 24 (1987) 51–60, <https://doi.org/10.1080/18811248.1987.9735774>.
- [25] S.A. Gallagher, G.J. McCarthy, Preparation and X-ray characterization of pollucite $(\text{CsAlSi}_5\text{O}_{12})$, *J. Inorg. Nucl. Chem.* 43 (1981) 1773–1777, [https://doi.org/10.1016/0022-1902\(81\)80382-X](https://doi.org/10.1016/0022-1902(81)80382-X).
- [26] J.H. Yang, H.S. Park, Y.Z. Cho, Immobilization of Cs-trapping ceramic filters within glass-ceramic waste forms, *Ann. Nucl. Energy* 110 (2017) 1121–1126, <https://doi.org/10.1016/j.anucene.2017.08.051>.
- [27] Y. Yokomori, S. Idaka, The crystal structure of analcime, *Microporous Mesoporous Mater.* 21 (1998) 365–370, [https://doi.org/10.1016/S1387-1811\(98\)00019-5](https://doi.org/10.1016/S1387-1811(98)00019-5).
- [28] B.G. Ferraris, D.W. Jones, J. Yerkes, A neutron-diffraction study of the crystal structure of analcime, $\text{NaAlSi}_3\text{O}_6 \cdot \text{H}_2\text{O}$, *Zeitschrift Fur Krist* 135 (1972) 240–252.
- [29] R.M. Beger, The crystal structure and chemical composition of pollucite, *Zeitschrift Fur Krist. - New Cryst. Struct.* 129 (1969) 280–302, <https://doi.org/10.1524/zkri.1969.129.1-4.280>.
- [30] K. Yanagisawa, N. Yamasaki, N. Kozai, S. Muraoka, Leachability of waste form containing cesium produced by hydrothermal hot-pressing, *J. Nucl. Sci. Technol.* 27 (1990) 1072–1074, <https://doi.org/10.1080/18811248.1990.9731294>.
- [31] J.R. Ugal, M. Mustafa, A.A. Abdulhadi, Preparation of zeolite type 13X from locally available raw materials, *Iraqi J. Chem. Pet. Eng.* 9 (2008) 51–56.
- [32] R. Xu, W. Pang, J. Yu, Q. Huo, J. Chen, Chemistry of Zeolites and Related Porous Materials, John Wiley & Sons, 2010, <https://doi.org/10.1002/9780470822371>.
- [33] M. Omerasević, L. Matović, J. Ružić, Ž. Golubović, U. Jovanović, S. Mentus, V. Dondur, Safe trapping of cesium into pollucite structure by hot-pressing method, *J. Nucl. Mater.* 474 (2016) 35–44, <https://doi.org/10.1016/j.jnucmat.2016.03.006>.
- [34] R.C. Ewing, W.J. Weibert, F.W. Clinard, Radiation effects in nuclear waste forms for high-level radioactive waste, *Prog. Nucl. Energy* 29 (1995) 63–127.
- [35] F.A. Bannister, M.H. Hey, A chemical, optical, and X-ray study of nepheline and Kaliophilite, *Mineral. Mag. J. Mineral Soc.* 22 (1931) 569–608, <https://doi.org/10.1180/minmag.1931.022.134.03>.
- [36] G.D. Gatta, P. Cappelletti, B. de Gennaro, N. Rotiroti, A. Langella, New data on Cu-exchanged phillipsite: a multi-methodological study, *Phys. Chem. Miner.* 42 (2015) 723–733, <https://doi.org/10.1007/s00269-015-0757-6>.
- [37] A. Brundu, G. Cerri, Thermal transformation of Cs-clinoptilolite to $\text{CsAlSi}_5\text{O}_{12}$, *Microporous Mesoporous Mater.* 208 (2015) 44–49, <https://doi.org/10.1016/j.micromeso.2015.01.029>.
- [38] I.A. Breger, J.C. Chandler, P. Zubovic, An infrared study of water in heulandite and clinoptilolite, *Am. Mineral.* 55 (1970) 825–840.
- [39] M. Omerasević, J. Ružić, B.N. Vasiljević, Z. Bašcarević, D. Bučevac, J. Orlić, L. Matović, Transformation of Cs-exchanged clinoptilolite to $\text{CsAlSi}_5\text{O}_{12}$ by

- hot-pressing, *Ceram. Int.* 43 (2017) 13500–13504, <https://doi.org/10.1016/j.ceramint.2017.07.055>.
- [40] R. Dimitrijevic, V. Dondur, N. Petranovic, The high temperature synthesis of CsAlSiO_4 -ANA, polymorph in the system $\text{Cs}_2\text{O}-\text{Al}_2\text{O}_3-\text{SiO}_2$, *J. Solid State Chem.* 95 (1991) 335–345.
- [41] D.K. Teertstra, P. Cerny, R. Chapman, Compositional heterogeneity of pollucite from high grade Dyke, Maskwa lake, Southeastern Manitoba, *Can. Mineral.* 30 (1992) 687–697.
- [42] P.F. Becher, Crack bridging processes in toughened ceramics, in: *Toughening Mechanisms in Quasi-Brittle Materials*, Kluwer Academic Publishers, 1991, pp. 19–20.
- [43] H. Kada, M. Lachemi, N. Petrov, O. Bonneau, P.C. Aitcin, Determination of the coefficient of thermal expansion of high performance concrete from initial setting, *Mater. Struct.* 35 (2001) 35–41, <https://doi.org/10.1617/13684>.
- [44] I. Yanase, S. Tamai, S. Matsuura, H. Kobayashi, Fabrication of low thermal expansion porous body of cubic cesium-deficient type pollucite, *J. Eur. Ceram. Soc.* 25 (2005) 3173–3179, <https://doi.org/10.1016/j.jeurceramsoc.2004.06.020>.
- [45] T. Ota, I. Yamai, H. Suzuki, Thermal expansion of nepheline solid solutions in the system of $\text{Na}_{1-2x}\text{Ca}_x\text{AlSiO}_4$, *J. Mater. Sci. Lett.* 13 (1994) 393–394.